NAVAL POSTGRADUATE SCHOOL
Monterey, California

19971105 022

THESIS

> ### NUMERICAL SIMULATION OF FLOW INDUCED BY A SPINNING SPHERE USING SPECTRAL METHODS
>
> by
>
> Birol Zeybek
>
> March 1997
>
> Thesis Advisor: Ashok Gopinath

Approved for public release; distribution is unlimited.

<table>
<tr><td colspan="3"><h1>REPORT DOCUMENTATION PAGE</h1></td><td>Form Approved OMB No. 0704-0188</td></tr>
</table>

REPORT DOCUMENTATION PAGE			Form Approved OMB No. 0704-0188

1. AGENCY USE ONLY *(Leave blank)*	2. REPORT DATE March 1997	3. REPORT TYPE AND DATES COVERED Master's Thesis
4. TITLE AND SUBTITLE NUMERICAL SIMULATION OF FLOW INDUCED BY A SPINNING SPHERE USING SPECTRAL METHODS.		5. FUNDING NUMBERS
6. AUTHOR(S) Zeybek, Birol		
7. PERFORMING ORGANIZATION NAME(S) AND ADDRESS(ES) Naval Postgraduate School Monterey, CA 93943-5000		8. PERFORMING ORGANIZATION REPORT NUMBER
9. SPONSORING/MONITORING AGENCY NAME(S) AND ADDRESS(ES)		10. SPONSORING/MONITORING AGENCY REPORT NUMBER
11. SUPPLEMENTARY NOTES The views expressed in this thesis are those of the author and do not reflect the official policy or position of the Department of Defense or the U.S. Government.		
12a. DISTRIBUTION/AVAILABILITY STATEMENT Approved for public release; distribution is unlimited.		12b. DISTRIBUTION CODE

13. ABSTRACT *(maximum 200 words)*

A direct numerical simulation, based on spectral methods, has been used to investigate viscous, incompressible, steady, rotationally symmetric flow due to a sphere rotating with a constant angular velocity about a diameter. The equations of motion have been reduced to a set of three nonlinear second order partial differential equations in terms of the vorticity, the stream function and the azimuthal velocity. The calculations have been carried out for Reynolds numbers (Re) from the Stokes flow regime (low Re) to the boundary layer regime (high Re).

The numerical results clearly show how the Stokes flow behavior for low Reynolds numbers, and the boundary layer behavior for high Reynolds numbers, are approached in the appropriate limits. Besides showing the flow streamlines, results have been presented for the torque and the skin friction behavior. It is shown that the present results are in excellent agreement with both available experimental data, and previously obtained numerical data. The radial equatorial jet which develops with increasing Reynolds numbers has been observed as expected from boundary layer collision behavior. No separation was observed for the range of Reynolds numbers considered, even near the equator.

14. SUBJECT TERMS Spinning Sphere, Rotationally Symmetric Flow, Spectral Methods		15. NUMBER OF PAGES 59
		16. PRICE CODE

17. SECURITY CLASSIFICATION OF REPORT Unclassified	18. SECURITY CLASSIFICATION OF THIS PAGE Unclassified	19. SECURITY CLASSIFICATION OF ABSTRACT Unclassified	20. LIMITATION OF ABSTRACT UL

NSN 7540-01-280-5500

Standard Form 298 (Rev. 2-89)
Prescribed by ANSI Std. 239-18 298-102

NUMERICAL SIMULATION OF FLOW INDUCED BY A SPINNING SPHERE USING SPECTRAL METHODS

Birol Zeybek
Lieutenant Junior Grade, Turkish Navy
B.S., Turkish Naval Academy, 1991

Submitted in partial fulfillment of the
requirements for the degree of

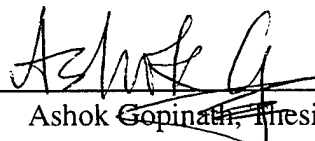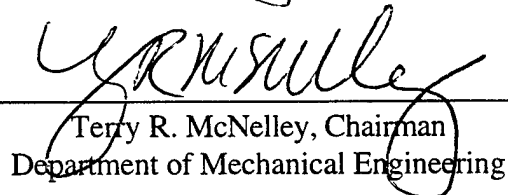## MASTER OF SCIENCE IN MECHANICAL ENGINEERING

from the

NAVAL POSTGRADUATE SCHOOL
March 1997

Author: _____

Birol Zeybek

Approved by: _____

Ashok Gopinath, Thesis Advisor

_____

Terry R. McNelley, Chairman
Department of Mechanical Engineering

iii

ABSTRACT

A direct numerical simulation, based on spectral methods, has been used to investigate viscous, incompressible, steady, rotationally symmetric flow due to a sphere rotating with a constant angular velocity about a diameter. The equations of motion have been reduced to a set of three nonlinear second order partial differential equations in terms of the vorticity, the stream function and the azimuthal velocity. The calculations have been carried out for Reynolds numbers (Re) from the Stokes flow regime (low Re) to the boundary layer regime (high Re).

The numerical results clearly show how the Stokes flow behavior for low Reynolds numbers, and the boundary layer behavior for high Reynolds numbers, are approached in the appropriate limits. Besides showing the flow streamlines, results have been presented for the torque and the skin friction behavior. It is shown that the present results are in excellent agreement with both available experimental data, and previously obtained numerical data. The radial equatorial jet which develops with increasing Reynolds numbers has been observed as expected from boundary layer collision behavior. No separation was observed for the range of Reynolds numbers considered, even near the equator.

TABLE OF CONTENTS

I. INTRODUCTION

The study of direct numerical simulation of steady viscous flow due to a sphere which rotates about a diameter with constant angular velocity in a fluid at rest has historically been the focus of a great deal of scientific attention. Most of the previous studies were based on finite-difference schemes.

In this study, a different numerical scheme based on spectral methods was used. The validity of the numerical method and the results were checked with the previous studies. Spectral methods have become increasingly popular in recent years, especially since the development of fast transform methods, with applications in numerical weather prediction, numerical simulation of laminar and turbulent flows and other problems where high accuracy is desired for complicated results.

The objective of this study is to compute the numerical simulation of a steady flow about a spinning sphere by using the spectral numerical methods. A Matlab program was developed by using spectral methods. However the method itself was not compared to the other methods used in previous studies. The reliability and validity of the numerical method were investigated to improve our current ability to compute and predict the evolution of flow for a particular geometry and conditions.

II. BACKGROUND STUDIES

The spectral method is based on the collocation method which appears to have been used first by Slater and Kantorovic in specific applications in 1934. It was developed as a general method for solving ordinary differential equations. This method was revived by Wrigt in 1964. The applications of Chebyshev polynomial expansions to the initial value problems were involved in these studies.

The spectral collocation method was applied to partial differential equations for spatially periodic problems by Kreiss and Oliger, who called it the Fourier method, and Orszag, who termed it "pseudospectral". These were the earliest applications of spectral collocation or the pseudospectral method. This approach was very attractive because of its application to variable-coefficient and even non-linear problems.

The Galerkin approach which depends on the same trial and test functions, was applied to a meteorological model by Silberman in 1954. This was the first serious application of spectral methods to PDEs. In 1970, Machenhauer and Rasmussen developed transform methods for evaluating convolution sums arising from quadratic non-linearity. Spectral Galerkin methods became practical for high resolution calculations of such non-linear problems. Applications in fluid dynamics were reviewed in the symposium proceedings edited by Voigt, Gottlieb and Hussaini in 1984.

For the problem of the flow induced by a spinning sphere being considered in this study, the flow behavior for small values of the Reynolds number, Stokes [Ref. 1], Lamb [Ref. 2], Bickley [Ref .3], Collins [Ref. 4], Thomas and Walters [Ref. 5], Ovseenko [Ref. 6], and Takagi [Ref. 7] have given theoretical results. For high Reynolds number, the boundary-layer equations have been studied by Howarth [Ref. 8], Nigam [Ref. 9], Stewartson [Ref. 10], Fox [Ref. 11], Banks [Refs. 12 & 13], Manohar [Ref. 14], and Singh [Ref. 15]. Over a large range of values of Reynolds number the flow has been investigated experimentally by Kobashi [Ref. 16], Bowden and Lord [Ref. 17], Kreith et al [Ref. 18], and Sawatzki [Ref. 19]. Another numerical method based on the use of

3

specialized techniques to obtain an approximation of the finite-difference form of the full partial differential equations was performed by Allen and Southwell [Ref. 20], Dennis [Refs. 21 & 22], Roscoe [Refs. 23 & 24], Spalding [Ref. 25] and Dennis, Ingham and Singh [Ref. 26].

III. GOVERNING EQUATIONS

A.   DERIVATION OF EQUATIONS

The governing equations for the problem are as follow;

$$\frac{\partial \mathbf{u}}{\partial t} + (\mathbf{u}.\nabla)\mathbf{u} = -\frac{1}{\rho}\nabla p + \nu\nabla^2\mathbf{u} \qquad (3.1) \text{ Momentum equation}$$

$$\nabla.\mathbf{u} = 0 \qquad (3.2) \text{ Continuity equation}$$

Define dimensionless variables;

$$r^* = \frac{r}{a} \qquad \mathbf{u}^* = \frac{\mathbf{u}}{U} \qquad \nabla p^* = \frac{\nabla p}{\rho U^2} \qquad \nabla^* = \frac{1}{a}\nabla$$

where   a : radius of the sphere,

   U : free stream velocity,

   ρ : density of the fluid,

   ν : kinematic viscosity of the fluid.

Introduce the dimensionless variables into Equation (3.1);

$$\frac{U\nu}{a^2}\frac{\partial \mathbf{u}^*}{\partial t} + \frac{U^2}{a}(\mathbf{u}^*.\nabla)\mathbf{u}^* = -\frac{1}{\rho}\frac{U^2}{a}\nabla p^* + \nu\frac{U}{a^2}\nabla^2\mathbf{u}^* \qquad (3.3)$$

Divide Equation (3.3) by $\dfrac{U.\nu}{a^2}$;

$$\frac{\partial \mathbf{u}^*}{\partial t} + \frac{U.a}{\nu}(\mathbf{u}^*.\nabla)\mathbf{u}^* = -\frac{U.a}{\nu}\nabla p^* + \nu\nabla^2\mathbf{u}^* \qquad (3.4)$$

Hereafter the superscript * will be omitted for nondimensional terms. Define the Reynolds number based on the diameter, $Re_d = \dfrac{U(2a)}{\nu}$, and take the Curl of Equation (3.4) to be able to eliminate the pressure term and introduce vorticity, $\omega = \nabla \times \mathbf{u}$ where

5

$$\omega = i_r \omega_r + i_\theta \omega_\theta + i_\phi \omega_\phi.$$

The transport equation for the Φ-component of the vorticity is

$$\frac{\partial}{\partial t}\omega_\phi i_\phi - \nabla \times (u \times \omega_\phi i_\phi) = \frac{2}{Re_d}\left(\nabla^2 - \frac{1}{r^2 \sin^2 \theta}\right)\omega_\phi i_\phi \qquad (3.5)$$

Convert the velocity in Equation (3.5) by defining the axisymmetric Stream function, ψ, and an "angular circulation", Ω.

$$u = \nabla \times \left[\frac{\psi}{r \sin \theta} i_\phi\right] + i_\phi \frac{\Omega}{r \sin \theta} \qquad \phi \text{ ; Azimuthal direction} \quad (3.6)$$

In spherical coordinates, Equation (3.6) is obtained as

$$u = \left[\frac{1}{r^2 \sin \theta}\frac{\partial \psi}{\partial \theta}\right]i_r - \left[\frac{1}{r \sin \theta}\frac{\partial \psi}{\partial r}\right]i_\theta + \frac{\Omega}{r \sin \theta}i_\phi \qquad (3.7)$$

where

$$u = u_r i_r + u_\theta i_\theta + u_\phi i_\phi \qquad (3.8)$$

In the free stream $\psi = \frac{1}{2}Ur^2 \sin^2 \theta$ or $\psi = \frac{1}{2}r^2 \sin^2 \theta$ in nondimensional form.

By using the definition of the stream function it can be shown that

$$\omega_\phi = \left[\frac{\partial^2 \psi}{\partial r^2} + \frac{1}{r^2}\frac{1}{\sin \theta}\frac{\partial}{\partial \theta}\left(\frac{1}{\sin \theta}\frac{\partial \psi}{\partial \theta}\right)\right]\left(\frac{-1}{r \sin \theta}\right) \qquad (3.9)$$

6

Define operator $\overline{D}^2$ as

$$\overline{D}^2 = \frac{\partial^2}{\partial r^2} + \frac{\sin\theta}{r^2}\frac{\partial}{\partial\theta}\left(\frac{1}{\sin\theta}\frac{\partial}{\partial\theta}\right) \tag{3.10}$$

to obtain the azimuthal component of the vorticity;

$$\omega_\Phi = -\frac{1}{r\sin\theta}\overline{D}^2\psi \tag{3.11}$$

Call $[\nabla\times(\mathbf{u}\times\omega_\Phi i_\Phi)].i_\Phi$ in Equation (3.5) nonlinear Term $G(r,\theta,t)$. By carrying out the calculations in spherical coordinates

$$\nabla\times(\mathbf{u}\times\omega_\Phi i_\Phi) = \frac{1}{r^3\sin\theta}\left[\frac{\partial(\psi,\overline{D}^2\psi)}{\partial(r,\mu)} + 2\overline{D}^2\psi L(\psi)\right] \tag{3.12}$$

is obtained, where

$$\mu = \cos\theta$$
$$L = \frac{\mu}{1-\mu^2}\frac{\partial}{\partial r} + \frac{1}{r}\frac{\partial}{\partial\mu} \tag{3.13}$$
$$\frac{\partial(z_1,z_2)}{\partial(x,y)} = \frac{\partial z_1}{\partial x}\frac{\partial z_2}{\partial y} - \frac{\partial z_1}{\partial y}\frac{\partial z_2}{\partial x}$$

Combine all terms to get

$$\frac{\partial}{\partial t}(\overline{D}^2\psi) + \frac{Re_d}{2}\frac{1}{r^2}\left[\frac{\partial(\psi,\overline{D}^2\psi)}{\partial(r,\mu)} + 2\overline{D}^2\psi L(\psi)\right] = \overline{D}^4\psi \tag{3.14}$$

7

Equation (3.14) is called the Vorticity-Stream function form of the Momentum Equation in axisymmetric spherical coordinate system. For computational purposes, which will become clear later, define a modified stream function $C(r,\theta,t)$, which is related to the usual Stokes stream function (ψ) by the relation;

$$\psi = rC \sin \theta \qquad (3.15)$$

Also for any function $f(r,\theta)$, define operator D^2 such that

$$\overline{D}^2 (fr \sin \theta) = r \sin \theta D^2 f$$

where

$$D^2 = \nabla^2 - \frac{1}{r^2 \sin^2 \theta} .$$

This gives

$$\omega_\phi = -D^2 C \qquad (3.16)$$

$$\mathbf{u} = \nabla \times (Ci_\phi) + \frac{\Omega}{r \sin \theta} i_\phi \qquad (3.17)$$

where

$$u_r = \frac{1}{r \sin \theta} \frac{\partial}{\partial \theta} (C \sin \theta)$$

$$u_\theta = -\frac{1}{r} \frac{\partial}{\partial r} (rC) \qquad (3.18)$$

$$u_\phi = \frac{\Omega}{r \sin \theta}$$

The modified stream function C is written as the sum $C = \overline{C} + c$, where $\overline{C} = 0$, (which is the prescribed quiescent free stream condition), and c represents the disturbance produced by the presence of the spinning sphere.

8

Returning to Equation (3.5), rearrange by multiplying both sides with $r^2 \dfrac{Re_d}{2}$,

$$r^2 \frac{Re_d}{2} \frac{\partial \omega}{\partial t} = r^2 \frac{Re_d}{2} G(r,\theta,t) + r^2 D^2 \omega \qquad (3.19)$$

$$r^2 D^2 C = -r^2 \omega \qquad (3.20)$$

where

$$G(r,\theta,t) = \left[\nabla \times (u \times \omega_\Phi i_\Phi) \right] \cdot i_\Phi \qquad (3.21)$$

Note that the operator D^2 is defined as

$$D^2 = \frac{1}{r^2} \frac{\partial}{\partial r}\left(r^2 \frac{\partial}{\partial r} \right) + \frac{1}{r^2 \sin^2 \theta} \frac{\partial}{\partial \theta}\left(\sin \theta \frac{\partial}{\partial \theta} \right) - \frac{1}{r^2 \sin^2 \theta} \qquad (3.22)$$

Divide $r^2 D^2$ in two parts which are D_r^2 and D_θ^2 respectively and obtain

$$r^2 D^2 = D_r^2 + \frac{1}{\sin^2 \theta} D_\theta^2 \qquad (3.23)$$

where D_r^2 and D_θ^2 are as defined in Chapter IV.

The nonlinear term in Equation (3.21), $G(r,\theta,t)$, consists of 8 terms. These are

$$-\frac{1}{r} \frac{\partial \omega_\Phi}{\partial r} \frac{\partial C}{\partial \theta} \qquad\qquad \frac{1}{r} \frac{\partial \omega_\Phi}{\partial \theta} \frac{\partial C}{\partial r} \qquad\qquad -\frac{Cot\theta}{r} \omega_\Phi \frac{\partial C}{\partial r} \qquad\qquad -\frac{Cot\theta}{r} C \frac{\partial \omega_\Phi}{\partial r}$$

$$\frac{\omega_\Phi}{r^2} \frac{\partial C}{\partial \theta} \qquad\qquad \frac{C}{r^2} \frac{\partial \omega_\Phi}{\partial \theta} \qquad\qquad 2u_\Phi \frac{Cot\theta}{r} \frac{\partial u_\Phi}{\partial r} \qquad\qquad -\frac{2u_\Phi}{r^2} \frac{\partial u_\Phi}{\partial \theta}$$

Time integration of vorticity equation (3.19) is accomplished through the use of an explicit second-order Adams-Bashforth scheme for the nonlinear terms and an implicit

9

second-order Crank-Nicolson scheme for the viscous and linear terms. The calculations are made in physical r-space and spectral θ-space. If we denote vorticity $\omega(r,t)$ as the vector of N sine series then the discretized form of Equation (3.19) is

$$r^2 \frac{Re_d}{2}\left[\frac{\omega_{t+\Delta t}-\omega_t}{\Delta t}\right] = r^2 \frac{Re_d}{2}\left[\alpha G_t + \beta G_{t-\Delta t}\right] + \left[D_r^2 + A\right]\left(\frac{\omega_t + \omega_{t+\Delta t}}{2}\right) \tag{3.24}$$

where α and β are suitably chosen weighting parameters in the implicit scheme.

Rearrange Equation (3.24) and obtain

$$\left[D_r^2 + A - r^2 \frac{Re_d}{\Delta t}\right]\omega_{t+\Delta t} = -\left[D_r^2 + A + r^2 \frac{Re_d}{\Delta t}\right]\omega_t - r^2 Re_d\left[\alpha G_t + \beta G_{t-\Delta t}\right] \tag{3.25}$$

where $\alpha = \dfrac{3}{2}$, $\beta = -\dfrac{1}{2}$ and $G = \left(\nabla \times (u \times \omega_\phi i_\phi)\right) \cdot i_\phi$

$$\left[D_r^2 + A\right]c(r, t+\Delta t) = -r^2\omega(r, t+\Delta t) \tag{3.26}$$

We find the governing equation for u_ϕ in same way:

$$\frac{\partial\Omega}{\partial t} + \frac{1}{r^2}\left[\frac{\partial(\Psi,\Omega)}{\partial(r,\cos\theta)}\right] = \frac{2}{Re_d}\overline{D}^2\Omega \tag{3.27}$$

where $\dfrac{\Omega}{r\sin\theta} = u_\phi$ and $C = \dfrac{\Psi}{r\sin\theta}$

and introduce $\overline{D}^2\Omega = \overline{D}^2\left(u_\phi r\sin\theta\right) = r\sin\theta D^2 u_\phi$ and divide each side by $(r\sin\theta)$

If Equation (3.27) is rearranged, the result is

$$\frac{\partial u_\phi}{\partial t} = -\frac{1}{r}\left[\frac{\partial(u_\theta,C)}{\partial(r,\theta)} + C^2\left\{\frac{\partial\left(\dfrac{u_\phi}{C}, Ln(r\sin\theta)\right)}{\partial(r,\theta)}\right\}\right] + \frac{2}{Re_d}D^2 u_\phi \tag{3.28}$$

10

The nonlinear term in Equation (3.28) is called H(r,θ,t) and consists of

$$-\frac{1}{r}\frac{\partial u_\Phi}{\partial r}\frac{\partial C}{\partial \theta}$$

$$\frac{1}{r}\frac{\partial u_\Phi}{\partial \theta}\frac{\partial C}{\partial r}$$

$$\frac{Cot\theta}{r}u_\Phi\frac{\partial C}{\partial r}$$

$$-\frac{Cot\theta}{r}C\frac{\partial u_\Phi}{\partial r}$$

$$-\frac{u_\Phi}{r^2}\frac{\partial C}{\partial \theta}$$

$$\frac{C}{r^2}\frac{\partial u_\Phi}{\partial \theta}$$

u_Φ is written as the sum of two parts: potential and disturbance parts,

$$u_\Phi = \overline{u}_\Phi + u_\Phi' \qquad \text{where} \qquad \overline{u}_\Phi = \frac{Sin\theta}{r^2} \quad \text{is the Stokes flow}$$

solution which satisfies $D^2\overline{u}_\Phi = 0$. The final form of Equation (3.28) is

$$\frac{\partial u_\Phi'}{\partial t} = H(r,\theta,t) + \frac{2}{Re_d}D^2(u_\Phi') \tag{3.29}$$

$$\frac{u_\Phi'(t+\Delta t) - u_\Phi'(t)}{\Delta t} = \frac{1}{2}[3H(t) - H(t-\Delta t)] + \frac{2D^2}{Re_d}\left[\frac{u_\Phi'(t) + u_\Phi'(t+\Delta t)}{2}\right] \tag{3.30}$$

$$u_\Phi'(t+\Delta t)\left[\frac{r^2 Re_d}{2\Delta t} - \frac{r^2 D^2}{2}\right] = u_\Phi'(t)\left[\frac{r^2 Re_d}{2\Delta t} + \frac{r^2 D^2}{2}\right] + \frac{r^2 Re_d}{4}[3H(t) - H(t-\Delta t)] \tag{3.31}$$

$$\left[Dr^2 + A - \frac{Re_d r^2}{\Delta t}\right]u_\Phi'(t+\Delta t) = -\left[Dr^2 + A + \frac{r^2 Re_d}{\Delta t}\right]u_\Phi'(t) - \frac{r^2 Re_d}{2}[3H(t) - H(t-\Delta t)] \tag{3.32}$$

11

B.   BOUNDARY CONDITIONS

The boundary conditions for the numerical scheme are

$$c = -\overline{C} = 0 \qquad \frac{\partial c}{\partial r} = -\frac{\partial \overline{C}}{\partial r} = 0 \qquad u'_\phi = 0 \quad \text{at } r=1 \qquad (3.33)$$

$$c = 0 \quad \omega = 0 \quad u_\phi = 0 \quad \text{at } r = r_\infty \qquad (3.34)$$

The Neumann Boundary Conditions in Equation (3.33) are handled with the Green's Function Method that will be explained later. Zero boundary conditions in the θ direction are automatically satisfied with the choice of the sine expansions.

12

IV. METHOD OF SOLUTION

A. NUMERICAL METHOD

A pseudospectral or collocation method based on the technique developed by Marcus & Tuckerman [Ref. 29], is used to solve the equations of motion in time. Spectral methods may be viewed as an extreme development of weighted residual (MWR) which is generally used in a discretization scheme for differential methods. The trial functions and test functions are chosen as infinitely differentiable global functions. This is one of the features which distinguish spectral methods from finite-element and finite-difference methods. A pseudospectral transform method is used in this study. The approach taken in the transform method is to use the Fast Fourier Transform (FFT) to transform the functions to spectral space or Inverse Fast Fourier Transform (IFFT) to transform the equations to physical space.

A physical process can be described either in time domain, by the values of the same h as a function of t, e.g., h(t), or else in frequency domain, where the process is specified by giving its amplitude, H, as a function of frequency f, that is H(f), with $-\infty < f < \infty$. So once it is known whether the function is either odd or even, this information can be used in transformations. If h(t) is real and even then H(f) is real and even, if h(t) is real and odd then H(f) is imaginary and odd. It is necessary to go back and forth between these two domains by means of Fourier transform equations. As explained below, odd functions, using sine series expansions for ω, c and u_Φ, are used. The same properties are valid for derivatives of these expansions. Using these properties will increase computational efficiency.

Functions are presented both in spectral space as a finite series of basis functions and by values at collocation grid points in physical space. The vorticity, ω, the modified stream function, C, and the velocity in the Φ direction, u_Φ, are expanded as Chebyshev polynomials in the radial direction and as sine series in the transverse direction. The products and the derivatives in radial direction are done in physical space while the

13

derivatives in transverse direction are obtained in spectral space. Since each sine term in the expansion satisfies the homogenous θ boundary conditions ($\omega = 0$, $\Psi = 0$, $u_\phi = 0$ at $\theta = 0, \pi$) exactly, no further θ boundary conditions need to be applied.

In general let a variable, say ω, be expressed as

$$\omega(r,\theta,t) = \sum_{n=1}^{N} \omega_n(z,t)\mathrm{Sin}(\theta_n) \tag{4.1a}$$

with

$$\omega_n(z,t) = \sum_{m=0}^{M} \omega_{mn}(t)T_m(z) \tag{4.1b}$$

where $T_m(z)$ is Chebyshev Polynomial with $-1 \leq z \leq 1$

$$\theta_n = \frac{n\pi}{N+1} \qquad n = 1,2,...N \tag{4.2}$$

$$z = \mathrm{Cos}\left(\frac{m\pi}{M}\right) \qquad m = 0,1,...M \tag{4.3}$$

An algebraic map is used to map the radial interval $1 \leq r \leq r_\infty$ to the interval $-1 \leq z \leq 1$ where

$$r = 1 + L\frac{1+z}{b-z}, \quad |z| \leq 1 \tag{4.4}$$

with $\quad b = 1 + \dfrac{2L}{r_\infty - r_o} \quad$ (Note that $r_o = 1$, which is the surface of the sphere.)

L is a scaling parameter which is used to map the radial interval to the z-interval. A finite, but large outer r_∞, was chosen to avoid regularity problems in the radial differentiation.

The sine expansions (4.1a) for ω, C and u_ϕ satisfy the homogenous θ boundary conditions and match exactly the periodicity and symmetry conditions in θ. The solution of the elliptic equation (3.20) is required to obtain the modified stream function, C, from vorticity ω at any time level. Following [Ref. 29], separable derivative operators, D_r^2 and D_θ^2, are defined as

14

$$r^2 D^2 = D_r^2 + \frac{1}{\sin^2 \theta} D_\theta^2 \tag{4.5}$$

where

$$D_r^2 = \frac{\partial}{\partial r}\left(r^2 \frac{\partial}{\partial r}\right)$$

$$D_\theta^2 = \left[\sin\theta \frac{\partial}{\partial\theta}\left(\sin\theta \frac{\partial}{\partial\theta}\right) - 1\right] \tag{4.6}$$

In spectral θ-space the effect of operator $D_\theta{}^2$ at any fixed radial location (physical r-space) can be written as

$$D_\theta^2 . f(\theta) = \left[\sin^2\theta \frac{\partial^2}{\partial\theta^2} + \sin\theta.\cos\theta \frac{\partial}{\partial\theta} - 1\right] \Sigma f_j \sin(j\theta)$$

$$\ldots = \sum_{j=1}^{N} f_j \left[-(1 + \tfrac{1}{2} j^2)\sin(j\theta) + \tfrac{1}{4} j(1+j)\sin(2\theta + j\theta) + \tfrac{1}{4} j(1-j)\sin(2\theta - j\theta)\right] \tag{4.7}$$

If this expression is written in the form of $D_\theta^2 f(\theta) = \left[S_{ij}\right] f_j$

$$S_{ij} = \begin{cases} \dfrac{(i-2)(i-1)}{4} & i = j+2 \\[2mm] -1 - \dfrac{i^2}{2} & i = j \\[2mm] \dfrac{(i+2)(i+1)}{4} & i = j-2 \\[2mm] 0 & \text{otherwise} \end{cases} \tag{4.8}$$

is obtained.

This matrix is NxN if the representation for $D_\theta^2 f$ is truncated to N Fourier terms. Similarly, the operation of multiplying a function $f(\theta)$ by $\sin^{-2}(\theta)$ produces another NxN matrix which is called A matrix where the only non-zero terms are

$$A_{ij} = \begin{cases} a1(i) = -i(i+1) & i = j \\ a2(i) = -2i & i < j, i+j = \text{even} \end{cases} \tag{4.9}$$

15

Time integration of the equations are obtained by using the scheme which is explained in Chapter III.

The nonlinear terms, G and H, have to be carefully handled by transforming the spectral coefficients to physical space first, then multiplying the terms in physical space, and finally transforming the result of these products back to spectral space.

The radial derivatives are evaluated by collocation methods and expressed as matrix operations on the vector of function values at the grid points in physical r-space. For (M+1) collocation points, we introduce the (M+1)x(M+1) matrix operation, that is

$$D^{(1)}(n) = D_r^2 + \left[a(1) - \frac{Re}{\Delta t} r^2 \right] I \tag{4.10}$$

where, I is the identity matrix. The operator $[D_r^2 - r^2(Re/\Delta t) + A]$ in (3.25) and (3.32) may now be written in block matrix form as

$$\begin{bmatrix} D^{(1)}(1) & 0 & a2(1)I & 0 & \dots \\ 0 & D^{(1)}(2) & 0 & a2(2)I & \dots \\ 0 & 0 & D^{(1)}(3) & 0 & \dots \\ 0 & 0 & 0 & D^{(1)}(4) & \dots \\ \dots & \dots & \dots & \dots & \dots \end{bmatrix} \tag{4.11}$$

This matrix acts on the vector of a length of (M+1)xN for vorticity coefficients. Equations (3.25) and (3.26) are upper triangular, block matrix problems in physical r-space and spectral θ-space that can be solved by any solver with the Dirichlet and the Neumann boundary conditions discussed below. The equation (3.32) is treated in the same manner and leads to an upper triangular, block matrix problem.

B.   GREEN'S FUNCTION METHOD

To enforce the radial boundary conditions in c-ω equations, (3.25) and (3.26), Green's Function Method has been developed which gives the correct boundary

conditions, (3.33) and (3.34), and allows the surface vorticity to develop naturally. If ω and c consist of two parts, homogenous and particular solutions, the following is written:

$$\omega = \omega_p + \sum_{j=1}^{N} \lambda_j \tilde{\omega}_j \quad \text{and} \quad c = c_p + \sum_{j=1}^{N} \lambda_j \tilde{c}_j \quad j=1,2,\ldots,N \quad (4.12)$$

If (4.12) is introduced into (3.25) and (3.26), the homogenous parts as follow with corresponding boundary conditions occur.

$$E^2 \tilde{\omega}_j (r,\theta) = 0 \quad (4.13) \qquad\qquad H^2 \tilde{c}_j = -r^2 \tilde{\omega}_j \qquad (4.14)$$

$$\tilde{\omega}_j (r = 1, \theta_i) = \delta_{ij} \qquad\qquad \tilde{c}_j (r = 1, \theta_i) = 0$$

$$\tilde{\omega}_j (r = \infty, \theta_i) = 0 \qquad\qquad \tilde{c}_j (r = \infty, \theta_i) = 0$$

The particular parts with corresponding boundary conditions are

$$E^2 \omega_p (r,\theta, t + \Delta t) = R(r,\theta,t) \quad (4.15) \qquad H^2 c_p (r,\theta, t + \Delta t) = -r^2 \omega_p (r,\theta,t) \qquad (4.16)$$

$$\omega_p (r = 1, \theta) = 0 \qquad\qquad\qquad c_p (r = 1, \theta) = -\overline{C}|_{r=1}$$

$$\omega_p (r = \infty, \theta) = 0 \qquad\qquad\qquad c_p (r = \infty, \theta) = 0$$

E^2 and H^2 are obtained from the block matrix defined in (4.11)

To find λ,

$$\frac{\partial c}{\partial r}|_{r=1} = -\frac{\partial \overline{C}}{\partial r}|_{r=1} \qquad\qquad (4.17)$$

is enforced.

17

If (4.12) is substituted into (4.17),

$$\frac{\partial c_p}{\partial r}\Big|_{r=1,\theta_i} + \sum_{j=1}^{N} \frac{\partial \tilde{c}_j}{\partial r}\Big|_{r=1,\theta_i} \lambda_j = -\frac{\partial \overline{C}}{\partial r}\Big|_{r=1,\theta_i} \tag{4.18}$$

is obtained.

Allow $\left[-\dfrac{\partial \overline{C}}{\partial r} - \dfrac{\partial c_p}{\partial r}\right]_{r=1,\theta_i} = H_i$ and $\dfrac{\partial \tilde{c}_j}{\partial r}\Big|_{r=1,\theta_i} = A_{ij}$ (4.19)

Finally from (4.18) and (4.19), $H_i = \displaystyle\sum_{j=1}^{N} A_{ij}\lambda_j$ occurs and we solve for λ_j as $\lambda = A^{-1}H$.

These λ values can now be used in Equation (4.12) to arrive at the values of ω and c.

18

V. RESULTS AND DISCUSSION

Numerical calculations were performed for following parameters.

Re	M	N	L	r_∞	dt
2	64	64	7	150	0.05
4	64	64	6	140	0.05
10	64	64	4	130	0.03
20	64	64	4	125	0.05
40	64	64	4	125	0.05
60	64	64	4	100	0.03
80	64	64	3	70	0.03
100	64	64	2	40	0.01
150	64	64	2	30	0.03
175	64	64	2	25	0.03
200	64	64	2	20	0.05
1000	64	64	1	17	0.01
2000	64	64	0.6	14	0.01
3000	120	128	1.5	15	0.01
5000	128	128	1	8	0.01

Table 1. Parameters Used in Numerical Calculations

One of the main problems associated with many investigations that deal with complete numerical solution of Navier Stokes equations is the behavior of numerical scheme at high Reynolds numbers. It was found here that numerical results could be obtained for higher values of Reynolds numbers. For computational purposes, the results for Reynolds numbers up to 5000 are presented.

19

For comparison, T (Torque) is defined as

$$T = \int_{S,r=1} \sigma^*_{r\Phi} r^* Sin\theta dS^* \tag{5.1}$$

If (5.1) is nondimensionalized, the following occurs:

$$\frac{T}{2\pi a^2 \rho v V} = \int_0^\pi \sigma_{r\Phi} Sin^2\theta d\theta \quad , \text{ where } \quad \sigma_{r\Phi} = r\frac{\partial}{\partial r}\left(\frac{u_\Phi}{r}\right) = \frac{\partial u_\Phi}{\partial r} - \frac{u_\Phi}{r}\bigg|_{r=1} \tag{5.2}$$

The small mapping parameter, L, with increasing Reynolds number provides a finer grid in the boundary layer. The re-circulation of the flow near the equator is another important result of a spinning sphere which will be explained later. Since most of the sign changes in velocity profiles occur in this region, decreasing L much below one is not a solution to gain some additional grid points in the boundary layer for high values of Reynolds number because finer grid near the sphere means coarser grid in the outer region.

Several solutions for large Reynolds numbers have been obtained by integrating numerically the boundary layer equations found in [Ref. 13] which gives

$$M = \frac{6.48}{Re_a^{1/2}}, \quad \text{where } Re_a = \frac{a^2\omega}{v} \tag{5.3}$$

There are some other investigations that recommend a different numerical factor such as 5.95 [Ref. 8], 6.54 [Ref. 12] and 6.53 [Ref. 14]. In [Ref. 26], Equation (5.3) was modified as

$$M = \frac{6.48}{Re_a^{1/2}} + \frac{31}{Re_a} \tag{5.4}$$

The Constants 6.48 and 31 in Equation (5.4) are for Reynolds numbers based on radius; these constants should be modified to 9.16 and 62 respectively for Reynolds numbers based on diameter as in this study.

20

Re_d	Takagi [Ref. 7]	Dennis, and Singh [Ref. 20]	Banks [Ref. 13]	Equation (5.4)	Dennis, and Singh [Ref. 26]	Present
2	50.307	50.309	6.48	37.480	50.305	50.31
4	25.216	25.218	4.58	20.082	25.216	25.23
20	5.401	5.399	2.05	5.149	5.398	5.40
40		3.048	1.45	2.999	3.048	3.02
100		1.554	0.916	1.496	1.554	1.54
200		0.966	0.648	0.958	0.966	0.96
1000			0.290	0.352	0.348	0.35
2000			0.205	0.236	0.234	0.23
3000			0.167	0.188		0.19
5000			0.129	0.142		0.14

Table 2. Nondimensional Torque (M) at Different Reynolds Numbers

Figure 1 shows the variation of nondimensional torque with Reynolds numbers. It is seen that as the Reynolds number increases the general trend is quite consistent with the boundary layer solution given in [Ref. 13].
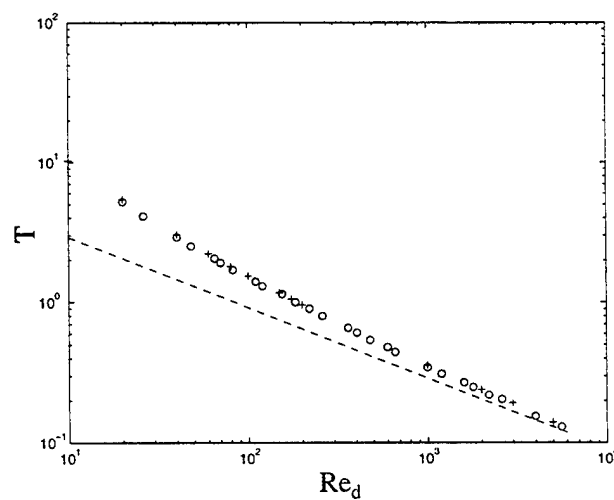

Figure 1. ---, Banks [Ref. 13]; o, Sawatzki [Ref. 19]; +, Present

Figure 2 and Figure 3 show the transverse and azimuthal components of the dimensionless skin friction on the sphere, respectively. As it is in Figure 1, the higher Reynolds number, the closer it is to the boundary layer solution. Transverse and azimuthal components of dimensionless skin friction are defined as

$$\tau_\theta = \left(\frac{2}{Re_d}\right)^{1/2}\left(\frac{\partial u_\theta}{\partial r}\right)_{r=1} \tag{5.5}$$

$$\tau_\Phi = \left(\frac{2}{Re_d}\right)^{1/2}\left(\frac{\partial u_\Phi}{\partial r}\right)_{r=1} \tag{5.6}$$

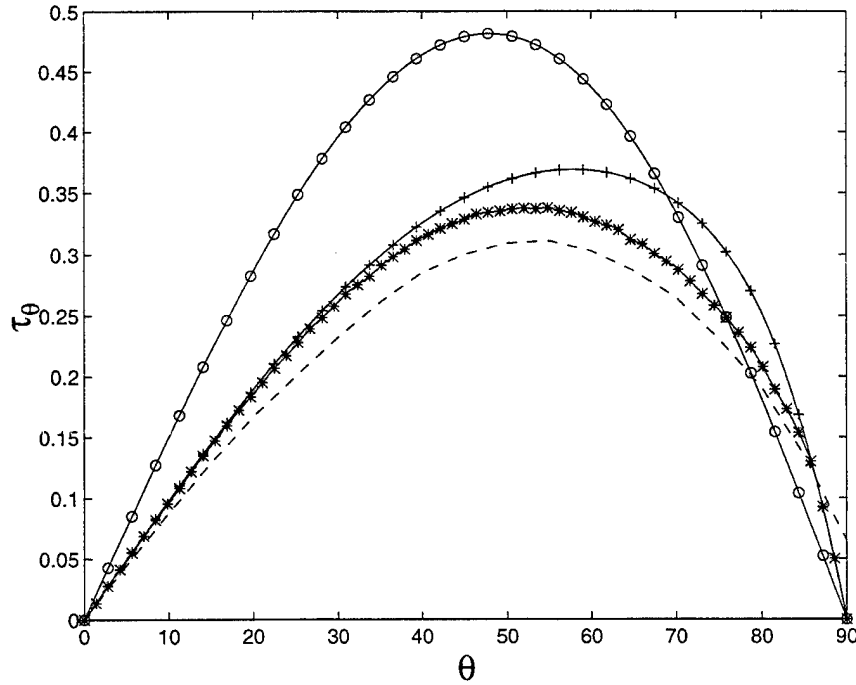**Figure 2.** Transverse Component of Skin Friction ; ---, Banks [Ref. 13] o, Re$_d$=20; +, Re$_d$=200; *, Re$_d$=3000
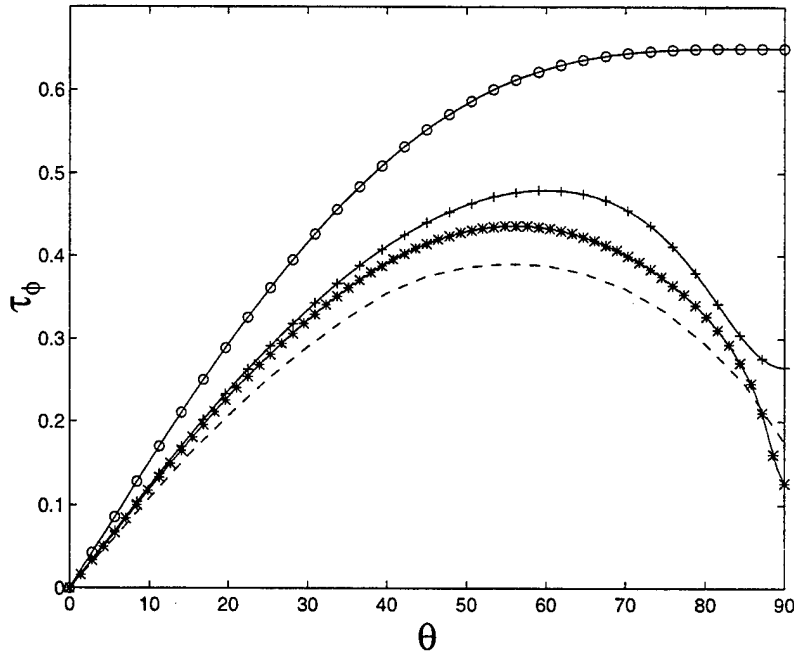
22

Figure 3. Azimuthal Component of Skin Friction; ---, Banks [Ref. 13]
o, $Re_d=20$; +, $Re_d=200$; *, $Re_d=3000$

Present results agree well with the boundary layer solution near the pole but this is not so for the equator region. This is because the boundary layer solution is obtained by integrating parabolic partial differential equations from $\theta=0$ with known initial conditions and the solution near the equator is determined from this procedure. Thus, it does not satisfy the physical boundary conditions.

Since a finite r_∞ is used and the modified stream function is forced to be zero at r_∞ and on the sphere, a spurious re-circulating region of extremely weak flow (relative magnitude $\approx 10^{-7}$) is introduced to account for the continuity in the flow domain. The inflow at the pole changes to an outflow at the equator. The angular position of this change depends on Re but does not vary greatly in terms of radial distance from the sphere. However, the general trend is to get closer to the sphere with increasing Reynolds numbers. Figure 4 shows the stream lines in symmetric plane for different values of Reynolds numbers.
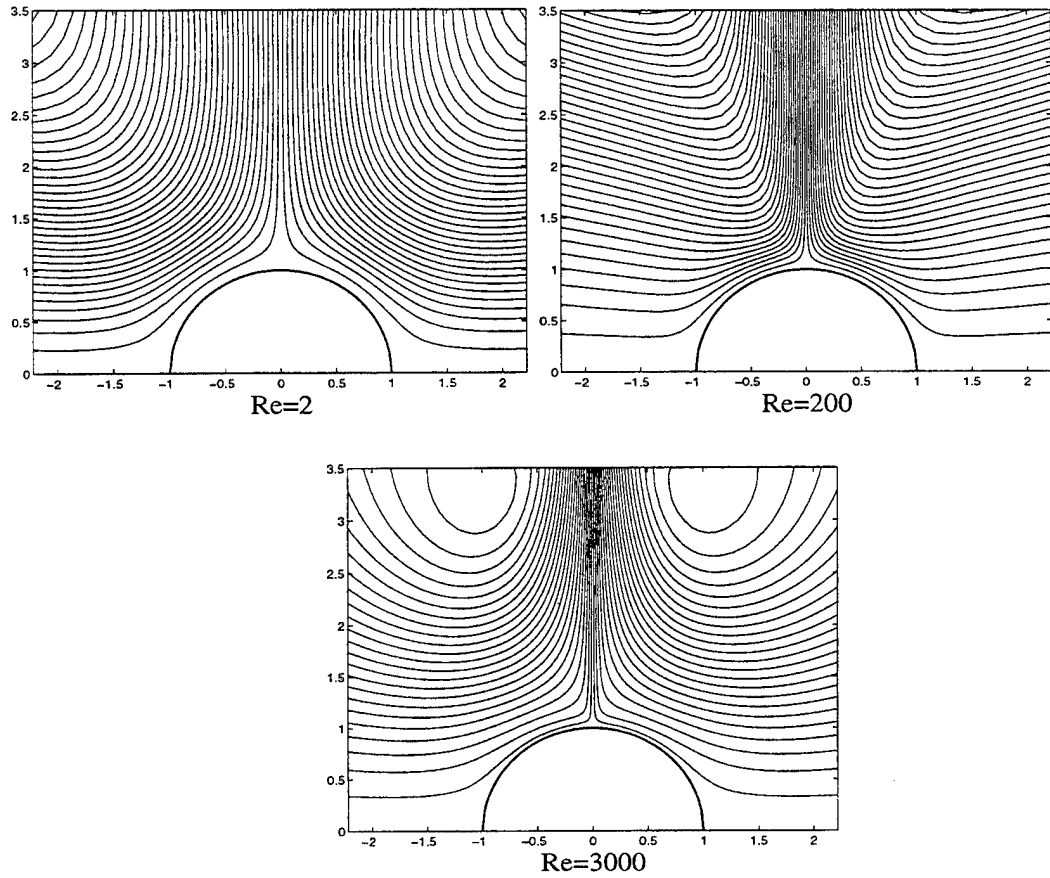
Figure 4. Stream Lines for Various Re

In Figure 5, the jet effect can be easily seen at the equator for two different Reynolds numbers. The darker color represents the regions where the magnitude of dimensionless velocity in the symmetric plane is higher. The reference velocity in Figure 5 is the velocity in the azimuthal direction on the sphere which has a value of unity.
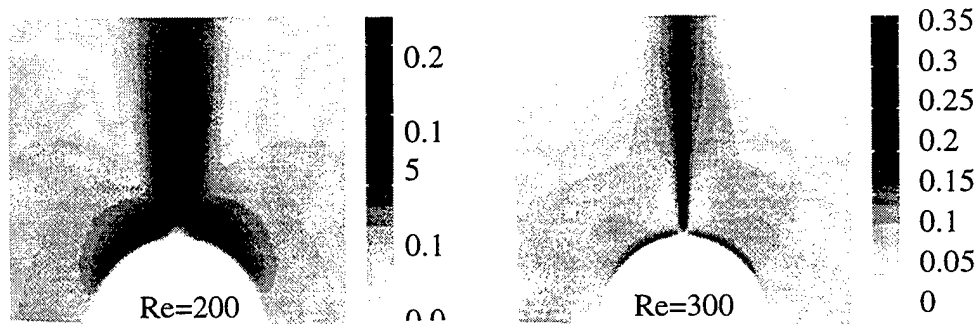

Figure 5. Jet Effect at Equator

24

Figure 6a and Figure 6b show the experimental flow visualization obtained by F. P. Bowden and R. G. Lord [Ref. 17], and present numerical solution for $Re_d=3300$ respectively. Note that, unlike Figure5, the velocity fields in Figure 6a and Figure 6b are in 3-D. As it is seen there is a reasonable resemblance between experimental and numerically obtained pictures. In the experiment, the sphere was levitated by means of a magnetic field. It was noted in [Ref. 17] that, because of this magnetic field, there is a slight upward convection current so the smoke rises slowly; this explains why the top half of the picture is white and the bottom half black. Note also that, the length of the radial jet is relatively shorter in Figure 6a. This behavior can be explained by the presence of possible shear turbulence in the radial jet for high Reynolds numbers causing the laminar jet behavior to disintegrate. Since the present results are obtained by means of a numerical solution without any kind of turbulence modeling, there is no effect of turbulence in our cases, even for higher Reynolds numbers.

Figure 6a. Smoke Picture of the Boundary Layer Flow for Re=3300. (From Ref. 17)

Figure 6b. Numerical Picture of the Boundary Layer Flow for Re=3300.

25

In the boundary layer approximation, it is assumed that the velocity profile in the boundary layer just before the equator is the same as the one at the start of boundary collision. This assumption yields zero radial velocity at $\theta = \pi/2$, near the sphere. From the results it is seen that radial velocity is not zero at the equator near the sphere. Figure 7 shows the variation of radial velocity with θ for Re = 200 at different radial distances from the sphere. Note that the maximum value of radial velocity occurs exactly at the equator. Besides, there is an inward flow at both poles. Although the maximum value of radial velocity at the equator increases with Reynolds numbers, the thickness of the region where a general outward flow from the equator can be discussed decreases.
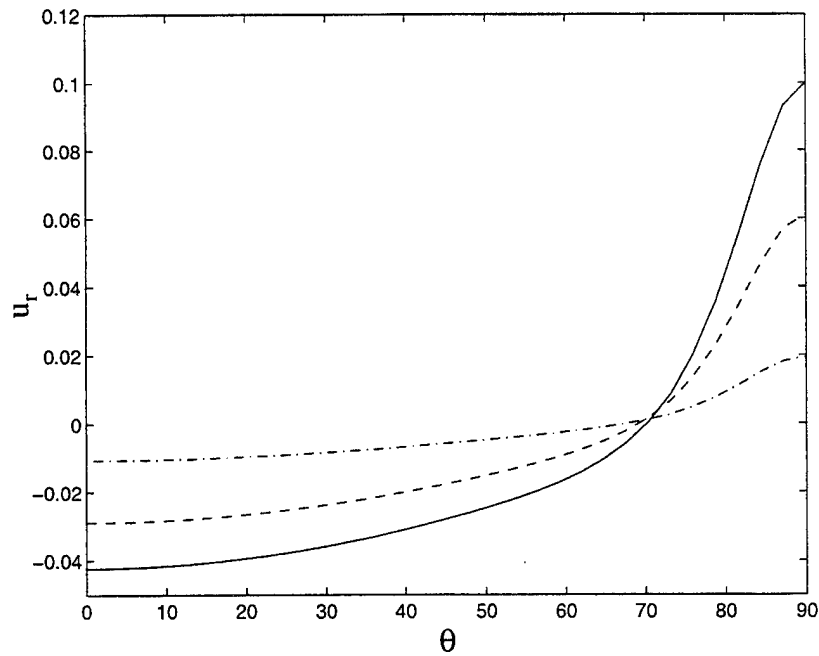

Figure 7. Variation of Radial Velocity with θ for Re = 200
-.-., r=1.0543; ---, r=1.1129; ___, r=1.1651

Figure 8 shows the variation of radial velocity with radial distance at the equator for different values of Reynolds numbers. Details of this swirling jet at the equator were given in [Ref. 27] and [Ref. 28].
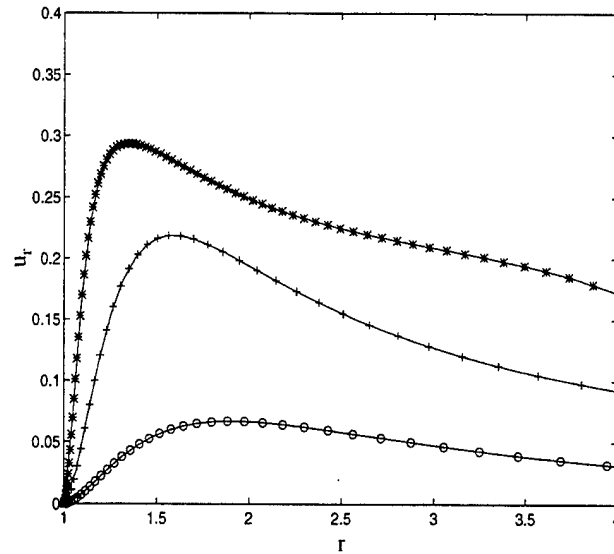
Figure 8. Variation of Radial Velocity with Radial Distance at $\theta=\pi/2$ o, Re=20
+, Re=200; *, Re=3000

Figure 9 shows the variation of dimensionless vorticity at the surface with θ at different Reynolds numbers. The interest of this figure is to show that no separation occurs over the surface of the sphere, since a sign change must take place as a point of separation is passed.

Figure 9. Variation of Dimensionless Vorticity with θ
o, Re=20; +, Re=200; *, Re=3000

27

It is known that the boundary layer solution to be approached as Reynolds numbers increases, especially near the poles, and it is accurate to $O(Re^{-1/2})$. Therefore, we might expect that $Re^{-1/2}\frac{\partial\omega}{\partial\theta}$ at $r = 1$ and $\theta = 0$ will be of the form
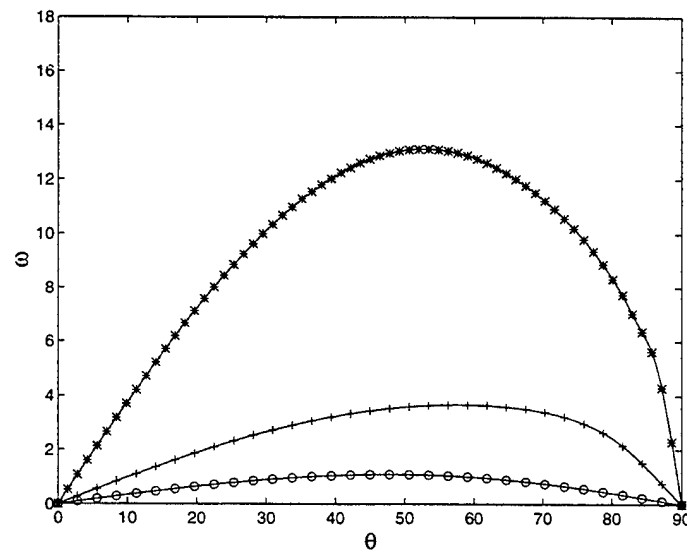
$$\frac{1}{Re_a^{1/2}}\left(\frac{\partial\omega}{\partial\theta}\right)_{\substack{r=1\\ \theta=0}} = A + B\,Re_a^{-1/2} \qquad (5.7)$$

where A and B are constants.

If $Re^{-1/2}\frac{\partial\omega}{\partial\theta}$ at $r = 1$ and $\theta = \pi/2$ is evaluted, it can be seen that this function is an increasing function of Re. It can be assumed that this expression is in the form of

$$\frac{1}{Re_a^{1/2}}\left(\frac{\partial\omega}{\partial\theta}\right)_{\substack{r=1\\ \theta=\pi/2}} = C\,Re_a^{\alpha} \qquad (5.8)$$

where C and α are constants.

The values of A, B, C and α were found by Dennis, Ingham and Singh [Ref. 26] to be 0.51, 0.56, 0.6 and ¼ respectively. The modified values of B and C for Reynolds numbers based on diameter are 0.79 and 0.5 respectively.

Re_d	$Re_d^{-1/2}\left(\frac{\partial\omega}{\partial\theta}\right)_{\substack{r=1\\ \theta=0}}$	$0.51 + \dfrac{0.79}{Re_d^{1/2}}$	$Re_d^{-1/2}\left(\frac{\partial\omega}{\partial\theta}\right)_{\substack{r=1\\ \theta=\pi/2}}$	$0.5\,Re_d^{1/4}$
10	0.695	0.760	0.43	0.89
20	0.639	0.687	0.806	1.06
50	0.597	0.622	1.15	1.33
100	0.576	0.589	1.50	1.58
200	0.552	0.566	1.79	1.88
1000	0.528	0.535		2.81
2000	0.523	0.528		3.34

Table 3. Calculated Values of $Re^{-1/2}\frac{\partial\omega}{\partial\theta}$ at $r = 1$, $\theta = 0$ and $r = 1$, $\theta = \pi/2$

VI. CONCLUSION AND RECOMMENDATIONS

In addition for the limiting cases of Re<<1 and Re>>1 for which Stokes flow and boundary layer solutions are available, the numerical results showed very good agreement with the those previously obtained by other numerical techniques. By changing some of the parameters such as r_∞ and L, the agreement with previous numerical results could be refined, although there is no proof that the other studies are correct within three decimal digits.

Choosing the mapping parameter, L, should be done carefully so as to have many grid points in the regions of large gradients. A much more powerful mapping should be determined that provides a finer grid in two completely different regions, namely the boundary layer region and the re-circulation region (which though spurious, must be captured accurately by the numerical method for other calculations).

A different FFT technique can be used that allows a number of grid points in the θ direction other than the ones that are a power of two. This would provide a relaxation in the choice of the number of grid points for different values of the Reynolds number which greatly affect the memory requirement. The problem is solved for $\theta = 0$ to $\theta = \pi$ with the aid of sine expansions. Since the problem is also symmetric with respect to $\pi/2$, by taking care of the even function properties it can only be solved for one quarter which simply doubles the grid points in θ direction with the same memory requirement.

The Green's Function Method that deals with the Neumann boundary conditions should not be considered a trivial detail and must be used to have a stable convergence process.

Obtained modified stream function values, C, can be easily used to solve the heat transfer problem due to convection from a spinning sphere. Derived additional energy equations are as follow

$$T(t+\Delta t)\left[r^2D^2 - Ec\frac{r^2}{\Delta t}\right] = -T(t)\left[r^2D^2 + Ec\frac{r^2}{\Delta t}\right] + Ec\frac{1}{2}\left[3K(t) - K(t-\Delta t)\right] \quad (6.1)$$

where $Ec = Pr\,Re$.

The nonlinear term, K, in Equation (6.1) consists of 5 parts

$$-\frac{\partial T}{\partial \theta}\frac{\partial C}{\partial r}r \qquad\qquad -\frac{\partial T}{\partial \theta}C \qquad\qquad \frac{\partial T}{\partial r}\frac{\partial C}{\partial \theta}r$$

$$CrCot(\theta)\frac{\partial T}{\partial r} \qquad\qquad -2Ec\frac{T}{Sin^2(\theta)}$$

Since, for forced convection only, Equation (6.1) is uncoupled from Navier Stokes equations, the steady state values of modified stream function, C, can be used in the energy equation after solving the fluid problem which decreases the additional memory requirement due to different block matrixes in Equation (6.1).

APPENDIX A. PROGRAM STRUCTURE

In the first part of the program, problem parameters were defined such as Re, dt, L, r_inf, M, N. Also calculations that are not dependent on time were performed in this part. To gain some additional memory D1, D2 and D3 were calculated with D_Bmat function and saved as diagonal elements only. Non-diagonal elements of these matrixes were included in each iteration.

Calculations showed that the matrix M1 (derivative operator in r direction) and consequently M3 and block matrixes that are diagonals of D1, D2 and D3 are ill-conditioned. To avoid numerical errors in solving equation systems, the Singular Value Decomposition method was used. Necessary SVD decomposition of the matrixes and calculations of ω and c that are used in the Green's Function Method were performed in this part. The built-in function in MATLAB, svd, was used for decomposition.

Time dependent calculations basically consist of four steps. In the first step, u_ϕ was calculated from Equation (3.32). In the second step, particular solutions of ω and c were found from Equations (3.25) and (3.26). In the third step, H, which is used in the Green's Function Method, was found and finally homogenous and the particular solutions were combined to get ω and c.

Most of the calculations were performed in spectral domain which is a feature of the numerical technique. Only nonlinear operations were done in physical domain. Nonlinear terms were calculated with the functions nonlin and nonlinsp for ω-c and u equations respectively.

A convergence criterion was not used in the program. For high Reynolds Number (above 200), some over-shooting occurs before steady state. This situation might have caused wrong results if a criterion was used. Instead, the results were checked during calculations and the program was terminated after seeing steady state.

31

Solsvd : This function was used to solve equations after SVD decomposition. The limit used in this function reduces numerical errors due to ill-condition matrixes by skipping close to singular values in each iteration.

Solsvd1 : Since this function was used for solving homogenous parts in the Green's Function Method and performed once before the time-loop, no limit was used in solsvd1.

Phy : This function was used for transformation of the variables from spectral domain to physical domain

Operat : Derivatives in θ direction in the spectral domain were performed with the function operat. Since these terms were used only in nonlinear terms, the output from this function is in the physical domain.

Variables that were used in the program are

L   : Mapping parameter.

Re   : Reynolds Number.

dt   : Time interval between iterations.

r_inf   : Outer boundary.

step   : Number of iterations.

N   : Number of grid points in θ direction.

M   : Number of grid points in r direction.

xcor, ycor : Cartesian coordinates of grid points with respect to the center of the sphere (used for the presentation of the results).

M1   : Derivative operator in r direction.

D1, D2, D3 : Matrixes defined as in Equation (4.11).

w   : Vorticity.

c   : Potential function as in Equation (3.15).

u   : Velocity component in Φ direction.

wtil, ctil : Homogenous part of the ω and c defined as in the Green's Function Method.

Aij, H, landa : Variables defined as in the Green's Function Method.

32

wp, cp : Particular solution of ω and c defined as in the Green's Function Method.

torq   : Dimensionless torque defined as in Equation (5.2).

APPENDIX B. PROGRAM CODES

%% define program parameters

```
clear all
global E M1 M2 M3
L=7;Re=2;dt=0.05;
r_inf=150;step=4500;
```

%% define grid points

```
N=32;n=[0:N-1]';
teta=n.*pi./N;
M=32;m=[0:M]';
z=cos(pi.*m./M);
b=1+2*L/(r_inf-1);
r=1+L.*(1+z)./(b-z);
global N M
xcor=cos(teta)*r';
ycor=sin(teta)*r';

E=emat(M);
disp('E matrix is done')
```

%% define M1,M2,M3

```
dz_dr=(b.*(L+r-1)-b.*(r-1)+L)./(L+r-1).^2;
B=diag(dz_dr);
M1=B*E;
R=diag(r);global R Re dt
M2=R*M1;
M3=R*(2.*eye(M+1)+M2)*M1;
```

%% define D1 D2 D3

```
[D1,D2,D3]=D_Bmat(M,N);
```

% define initial w c wp cp u

```
wp=zeros(M+1,N);cp=wp;w=wp;c=cp;
dum1=sin(teta)*(1./r.^2)';dum2=[dum1;zeros(1,M+1);-1.*flipud(dum1(2:N,:))];
dum3=fft(dum2);
```

```
u=wp;


%  define kmat (for teta der.) and cotteta (for nonlinear terms)

dum=ones(1,M+1);
kmat=n*dum;
cotteta=[0;cot(teta(2:N))]*dum;
global kmat cotteta teta


%  svd decomposition for D1 D3 and define rsquare (for nonlinear terms)

D1u=zeros(N*(M+1),M+1);
D1l=D1u;D1p=D1u;D3l=D1u;D3u=D1u;D3p=D1u;
rsquare=zeros(M+1,N);
for i=1:N
  bas=(i-1)*(M+1)+1;
  son=bas+M;
  rsquare(:,i)=r.^2;
  D1(bas,:)=[1 zeros(1,M)]; % modify D1 for w @ r=inf
  D1(son,:)=[zeros(1,M) 1]; % modify D1 for w @ r=1
  [D1l(bas:son,:),D1u(bas:son,:),D1p(bas:son,:)]=svd(D1(bas:son,:));
  D3(bas,:)=[1 zeros(1,M)]; % modify D3 for c @ r=inf
  D3(son,:)=[zeros(1,M) 1]; % modify D3 for c @ r=1
  [D3l(bas:son,:),D3u(bas:son,:),D3p(bas:son,:)]=svd(D3(bas:son,:));
end
global rsquare


%  define c_ c_teta c_r u_ u_teta u_r

c_=zeros(N,M+1);c_teta=c_;c_r=c_;
u_=1.*sin(teta)*(1./r.^2)';
u_teta=1.*cos(teta)*(1./r.^2)';
u_r=-2.*sin(teta)*(1./r.^3)';
global c_ c_teta c_r u_ u_teta u_r


% define c boundary at r=1

cbr1=zeros(1,N);


% begin green function wtil ctil

wtil=zeros(M+1,N^2);ctil=wtil;
```

```
for jj=1:N
  RR=zeros(M+1,N);
  dum1=[zeros(1,jj-1) 1 zeros(1,N-jj)];
  dum2=[dum1 0 -1.*fliplr(dum1(2:N))];
  dum3=fft(dum2);
  dum4=imag(dum3(1:N));
  RR(M+1,:)=dum4;
  wtil(:,jj*N)=solsvd1(D1l((N-1)*(M+1)+1:(N-1)*(M+1)+1+M,:),...
          D1u((N-1)*(M+1)+1:(N-1)*(M+1)+1+M,:),...
          D1p((N-1)*(M+1)+1:(N-1)*(M+1)+1+M,:),...
          RR(:,N));

  for i=N-1:-1:1
    sum=zeros(M+1,1);
    ii=(jj-1)*N+i;
    for j=i+1:N
        if rem(i+j,2)==2
            sum=sum+(-2*(i-1)).*wtil(:,(jj-1)*N+j);
        end
    sum(1)=0;
    sum(M+1)=0;
    end
    RR_=RR(:,i)-sum;

    wtil(:,ii)=solsvd1(D1l((i-1)*(M+1)+1:(i-1)*(M+1)+1+M,:),...
            D1u((i-1)*(M+1)+1:(i-1)*(M+1)+1+M,:),...
            D1p((i-1)*(M+1)+1:(i-1)*(M+1)+1+M,:),...
            RR_);

  end

  tempwtil=(-1.*rsquare).*wtil(:,(jj-1)*N+1:jj*N);
  tempwtil(M+1,:)=zeros(1,N);
  tempwtil(1,:)=zeros(1,N);
  ctil(:,jj*N)=solsvd1(D3l((N-1)*(M+1)+1:(N-1)*(M+1)+1+M,:),...
          D3u((N-1)*(M+1)+1:(N-1)*(M+1)+1+M,:),...
          D3p((N-1)*(M+1)+1:(N-1)*(M+1)+1+M,:),...
          tempwtil(:,N));

  for i=N-1:-1:1
    ii=(jj-1)*N+i;
    sum=zeros(M+1,1);
    for j=i+1:N
        if rem(i+j,2)==2
```

```
            sum=sum+(-2*(i-1)).*ctil(:,(jj-1)*N+j);
        end
    sum(1)=0;
    sum(M+1)=0;
    end
    wtil_=tempwtil(:,i)-sum;

    ctil(:,ii)=solsvd1(D3l((i-1)*(M+1)+1:(i-1)*(M+1)+1+M,:),...
            D3u((i-1)*(M+1)+1:(i-1)*(M+1)+1+M,:),...
            D3p((i-1)*(M+1)+1:(i-1)*(M+1)+1+M,:),...
            wtil_);
    end
end

% find Aij matrix

for jj=1:N
    blok=ctil(:,(jj-1)*N+1:jj*N);
    dum1=phy(blok')';
    dum2=(M1*dum1)';
    dum3=[dum2; zeros(1,M+1) ; -1.*flipud(dum2(2:N,:))];
    dum4=fft(dum3);dum5=imag(dum4(1:N,:));dum5=dum5';
    ctilr_1(jj,1:N)=dum5(M+1,:);
end

Aij=ctilr_1';

% find svd of Aij for landa solving

Aij(1,:)=[1 zeros(1,N-1)];
[Aiju,Aijs,Aijv]=svd(Aij);

% begin time loop

for ops=1:step

    if ops==1;prc=c;prw=w;pru=u;end

    %  find R1

    R1=zeros(M+1,N);
    R1(:,N)=D2((N-1)*(M+1)+1:(N-1)*(M+1)+1+M,:)*w(:,N);
    for i=N-1:-1:1
        summ=zeros(M+1,1);
```

```
    for j=i+1:N
        if rem(i+j,2)==2
            summ=summ+(-2*(i-1)).*w(:,j);
        end
    end
    R1(:,i)=D2((i-1)*(M+1)+1:(i-1)*(M+1)+1+M,:)*w(:,i)+summ;
end
R1=-1.*R1;

R1sp=zeros(M+1,N);
R1sp(:,N)=D2((N-1)*(M+1)+1:(N-1)*(M+1)+1+M,:)*u(:,N);
for i=N-1:-1:1
    summ=zeros(M+1,1);
    for j=i+1:N
        if rem(i+j,2)==2
            summ=summ+(-2*(i-1)).*u(:,j);
        end
    end
    R1sp(:,i)=D2((i-1)*(M+1)+1:(i-1)*(M+1)+1+M,:)*u(:,i)+summ;
end
R1sp=-1.*R1sp;

%   find R2sp

R2asp=nonlinsp(u,c);
R2bsp=nonlinsp(pru,prc);
R2sp=3/2.*R2asp-1/2.*R2bsp;
R2sp=(-1*Re).*rsquare.*R2sp;

Rtotsp=R1sp+R2sp;

%  find new u

%%  apply BC for u

Rtotsp(1,:)=zeros(1,N);   % BC for u=0 at r_inf
Rtotsp(M+1,:)=zeros(1,N);   % BC for u at r=1

u(:,N)=solsvd(D1l((N-1)*(M+1)+1:(N-1)*(M+1)+1+M,:),...
        D1u((N-1)*(M+1)+1:(N-1)*(M+1)+1+M,:),...
        D1p((N-1)*(M+1)+1:(N-1)*(M+1)+1+M,:),...
        Rtotsp(:,N));

for i=N-1:-1:1
```

```matlab
  sum=zeros(M+1,1);
  for j=i+1:N
      if rem(i+j,2)==2
         sum=sum+(-2*(i-1)).*u(:,j);
      end
  sum(1)=0;
  sum(M+1)=0;
  end
  Rtotsp_=Rtotsp(:,i)-sum;

  u(:,i)=solsvd(D1l((i-1)*(M+1)+1:(i-1)*(M+1)+1+M,:),...
         D1u((i-1)*(M+1)+1:(i-1)*(M+1)+1+M,:),...
         D1p((i-1)*(M+1)+1:(i-1)*(M+1)+1+M,:),...
          Rtotsp_);

end

%  find R2

R2a=nonlin(w,c,u);
R2b=nonlin(prw,prc,pru);
R2=3/2.*R2a-1/2.*R2b;
R2=(-1*Re).*rsquare.*R2;
Rtot=R1+R2;
prw=w;prc=c;pru=u;

%% green function solution

%  find new wp

%% apply BC for wp

Rtot(1,:)=zeros(1,N);   % BC for wp=0 at r_inf
Rtot(M+1,:)=zeros(1,N); % BC for wp=0 at r_1

wp(:,N)=solsvd(D1l((N-1)*(M+1)+1:(N-1)*(M+1)+1+M,:),...
        D1u((N-1)*(M+1)+1:(N-1)*(M+1)+1+M,:),...
        D1p((N-1)*(M+1)+1:(N-1)*(M+1)+1+M,:),...
        Rtot(:,N));

for i=N-1:-1:1
  sum=zeros(M+1,1);
  for j=i+1:N
      if rem(i+j,2)==2
```

```
            sum=sum+(-2*(i-1)).*wp(:,j);
        end
    sum(1)=0;
    sum(M+1)=0;
    end
    Rtot_=Rtot(:,i)-sum;

    wp(:,i)=solsvd(D1l((i-1)*(M+1)+1:(i-1)*(M+1)+1+M,:),...
            D1u((i-1)*(M+1)+1:(i-1)*(M+1)+1+M,:),...
            D1p((i-1)*(M+1)+1:(i-1)*(M+1)+1+M,:),...
            Rtot_);

end

%  solve for new cp

tempwp=-1.*rsquare.*wp;
tempwp(M+1,:)=cbr1; % BC for cp=-c_r at r_1 zero for pure spin
tempwp(1,:)=zeros(1,N); % BC for cp=0 at r_inf

cp(:,N)=solsvd(D3l((N-1)*(M+1)+1:(N-1)*(M+1)+1+M,:),...
        D3u((N-1)*(M+1)+1:(N-1)*(M+1)+1+M,:),...
        D3p((N-1)*(M+1)+1:(N-1)*(M+1)+1+M,:),...
        tempwp(:,N));

for i=N-1:-1:1
    sum=zeros(M+1,1);
    for j=i+1:N
        if rem(i+j,2)==2
            sum=sum+(-2*(i-1)).*cp(:,j);
        end
    sum(1)=0;
    sum(M+1)=0;
    end
    w_=tempwp(:,i)-sum;

    cp(:,i)=solsvd(D3l((i-1)*(M+1)+1:(i-1)*(M+1)+1+M,:),...
            D3u((i-1)*(M+1)+1:(i-1)*(M+1)+1+M,:),...
            D3p((i-1)*(M+1)+1:(i-1)*(M+1)+1+M,:),...
            w_);
end

%  find landa
%  find H
```

```
dum1=phy(cp')';
dum2=(M1*dum1)'; % NxM+1
dum3=-1.*c_r-dum2;
dum4=[dum3;zeros(1,M+1);-1.*flipud(dum3(2:N,:))];
dum5=fft(dum4);
dum6=imag(dum5(1:N,:));
dum6=dum6'; % M+1xN

H=dum6(M+1,:);H=H'; % Nx1
H(1)=0;
landa=solsvd(Aiju,Aijs,Aijv,H);

% find complete w & c

dum1c=zeros(M+1,N);dum1w=dum1c;
for jj=1:N
  blokc=ctil(:,(jj-1)*N+1:jj*N);
  blokw=wtil(:,(jj-1)*N+1:jj*N);
  dum2c=landa(jj).*blokc;
  dum2w=landa(jj).*blokw;
  dum1c=dum1c+dum2c;
  dum1w=dum1w+dum2w;
end

w=wp+dum1w;
c=cp+dum1c;

dum1=(phy(u')+u_)';
dum2=M1*dum1-dum1;
dum3=dum2(M+1,:)'.*(sin(teta).^2);
torq(ops)=-8*pi/Re*trapz(teta,dum3);
if ops>1
err(ops)=torq(ops)-torq(ops-1);
end

save tez4.mat u c w Re ops r_inf torq L N M dt;

end  % end of time loop

function [D1,D2,D3]=D_Bmat(M,N)
global M3 R dt Re
k=(M+1)*N;
D1=zeros(k,M+1);
```

```matlab
D2=zeros(k,M+1);
D3=zeros(k,M+1);
for i=1:N
  for j=i:N
   if i==j
     D1((i-1)*(M+1)+1:(i-1)*(M+1)+1+M,:)...
=M3+(-1*(i-1)*(i).*eye(M+1)-Re/dt.*R.^2);
     D2((i-1)*(M+1)+1:(i-1)*(M+1)+1+M,:)...
=M3+(-1*(i-1)*(i).*eye(M+1)+Re/dt.*R.^2);

     D3((i-1)*(M+1)+1:(i-1)*(M+1)+1+M,:)...
=M3+(-1*(i-1)*(i).*eye(M+1));
   end
  end
end


function E=emat(M)
E=zeros(M,M);
m=0:M;
z=cos(pi.*m./M);
for i=0:M
    for j=0:M
      if i~=j
        if ((i==0 I i==M) &  (j==0 I j==M)) I ((i~=0 & i~=M) &  (j~=0 & j~=M))
          c=1;else
        if (i==0 I i==M) &  (j~=0 & j~=M)
          c=2;else
        if (i~=0 & i~=M) &  (j==0 I j==M)
          c=1/2;end;end;end;
          E(i+1,j+1)=c*(-1)^(i+j)/(z(i+1)-z(j+1));
      else;
        if i==0
          E(i+1,j+1)=(2*M^2+1)/6;
        else
          if i==M
             E(i+1,j+1)=(2*M^2+1)/(-6);
          else
             E(i+1,j+1)=-1*z(j+1)/(2*(1-z(j+1)^2));
          end
        end
      end
    end
end
```

```
function R2=nonlin(w,c,u)
global kmat rsquare cotteta N M M1 c_ c_teta c_r teta u_ u_r u_teta
%  variable list
%
%  dw/dteta=non1 dc/dteta=non2 dw/dr=non3 dc/dr=non4 (in phy)
%  du/dteta=non5 du/dr=non6
%  transpose matrixes for colomn operations in teta direction
r=sqrt(rsquare)';w=w';c=c';u=u';
non1=operat(w);
non2=operat(c);
non5=operat(u);
wph=phy(w);cph=phy(c);uph=phy(u);
non3=[M1*wph']';
non4=[M1*cph']';non4(:,M+1)=-0.5.*sin(teta);
non6=[M1*uph']';
term1=-1./r.*non3.*(non2+c_teta);
term2=1./r.*non1.*(non4+c_r);
term3=-1.*cotteta./r.*wph.*(non4+c_r);
term4=-1.*cotteta./r.*non3.*(c_+cph);
term5=wph./rsquare'.*(non2+c_teta);
term6=(c_+cph)./rsquare'.*non1;
term7=1.*cotteta.*(non6+u_r).*(uph+u_).*2./r;
term8=-1.*(non5+u_teta).*2.*(uph+u_)./rsquare';
term0=term1+term2+term3+term4+term5+term6+term7+term8;
ter=[term0;zeros(1,M+1);-1.*flipud(term0(2:N,:))];
RR2=fft(ter);
R2=imag(RR2(1:N,:));R2=R2';

function R2sp=nonlinsp(u,c)
global kmat rsquare cotteta N M M1 c_ c_teta c_r teta u_ u_r u_teta
%  variable list
%
%  du/dteta=non1 dc/dteta=non2 du/dr=non3 dc/dr=non4 (in phy)
%  transpose matrixes for column operations in teta direction
r=sqrt(rsquare)';u=u';c=c';
non1=operat(u);
non2=operat(c);
uph=phy(u);cph=phy(c);
non3=[M1*uph']';
non4=[M1*cph']';
term1=-1./r.*(non3+u_r).*(non2+c_teta);
term2=1./r.*(non1+u_teta).*(non4+c_r);
term3=cotteta./r.*(uph+u_).*(non4+c_r);
term4=-1.*cotteta./r.*(non3+u_r).*(c_+cph);
```

```
term5=-1.*(uph+u_)./rsquare'.*(non2+c_teta);
term6=(c_+cph)./rsquare'.*(non1+u_teta);
term0=term1+term2+term3+term4+term5+term6;
ter=[term0;zeros(1,M+1);-1.*flipud(term0(2:N,:))];
RR2=fft(ter);
R2=imag(RR2(1:N,:));R2sp=R2';

function y=operat(x)
global N M kmat
re=zeros(N,M+1);
X=re+i.*x;
Y=i.*kmat.*X;
Y_ful=[Y;zeros(1,M+1);flipud(Y(2:N,:))];
y=ifft(Y_ful);
y=real(y(1:N,:));

function y=phy(x)
global N M
re=zeros(size(x));
X=re+i.*x;
Y_ful=[X;zeros(1,M+1);conj(flipud(X(2:N,:)))];
dum=ifft(Y_ful);
y=real(dum(1:N,:));

function y=solsvd(u,s,v,b)
w=diag(s);
wmin=max(w)*1e-12;
for i=1:length(w)
  if w(i)<wmin;ww(i)=0;else;ww(i)=1/w(i);end
end
www=diag(ww);
y=v*www*(u'*b);

function y=solsvd1(u,s,v,b)
w=diag(s);
for i=1:length(w)
  ww(i)=1/w(i);
end
www=diag(ww);
y=v*www*(u'*b);
```

LIST OF REFERENCES

1. G. G. STOKES, Trans. Camb. Phil. Soc., Vol. 8, 1845, pp.287.

2. H. LAMB, Hydrodynamics, 6th Ed., Cambridge, 1932, pp.588.

3. W. G. BICKLEY, Phil Mag., Vol. 28, 1938, pp.746.

4. W. D. COLLINS, Mathematika, Vol. 2, 1955, pp.42.

5. R. H. THOMAS and K. WALTERS, Q. Jl. Mech. Appl. Math., Vol. 17., 1964, pp.39.

6. I. G. OVSEENKO, Izv. Vyssh. Ucheb. Zaved. Math., Vol. 4, 1963, pp.129.

7. H. TAKAGI, J. Phys. Soc. Japan, Vol. 42,1977, pp.319.

8. L. HOWART, Phil. Mag., Vol. 42, 1951, pp.1308.

9. S. D. NIGAM, Z. Angew. Math. Phys., Vol. 5, 1954, pp.151.

10. K. STEWARTSON, In Boundary Layer Research Symposium Freiburg, Springer Berlin, 1958.

11. J. FOX, Boundary Layers on Rotating spheres and other Axisymmetric Shapes, N.A.S.A. TN D-2491, 1964.

12. W. H. H. BANKS, Q. Jl Mech. Appl. Math., Vol. 18, 1965, pp.320.

13. W. H. H. BANKS, Acta. Mech., Vol. 24., 1976, pp.273.

14. R. MANOHAR, Z. Angew. Math. Phys., Vol. 18, 1967, pp.320.

15. S. N. SING, Physics Fluids, Vol. 13, 1970, pp.2452.

16. Y. KOBASHI, J. Sci. Hiroshima Univ., Vol. 20, Japan ,1957, pp.3.

17. F. P. BOWDEN and R. G. LORD, Proc. R. Soc., Vol. 271, 1963, pp.143.

18. R. KREITH, L. G. ROBERTS, J. A. SULLIVAN and S. N. SINHA, Int. J. Heat Mass Transfer, Vol. 6, 1963, pp.881.

19. O. SAWATZKI, Acta. Mech., Vol. 9, 1970, pp.159.

20. D. N. DE G. ALLEN and R. V. SOUTHWELL, Q. Jl Mech. Appl. Math, Vol. 8, 1955, pp.129.

21. S. C. R. DENNIS, Ibid, Vol 13, 1960, pp.487.

22. S. C. R. DENNIS, Lecture Notes in Physics, 1973.

23. D. F. ROSCOE, J. Inst. Maths. Applics., Vol. 16, 1975, pp291.

24. D. F. ROSCOE, Int. J. Num. Math. Engin, 1299, 1972.

25. D. B. SPALDING, Ibid, Vol. 4, 1972, pp.551.

26. S. C. R. DENNIS, D. B. INGHAM and S. N. SINGH, Q. Jl Mech. Appl. Math., Vol. 34, 1981.

27. N. RILEY, Q. Jl Mech. App. Math., Vol. 15, 1962, pp.435.

28. P. D. RICHARDSON, Int. J. Heat Mass Transfer, Vol. 19, 1976, pp.1189.

29. P.S. MARCUS, L.S. TUCKERMAN, JFM, Vol. 185, 1987, pp.1-30.

INITIAL DISTRIBUTION LIST

No. Copies

1. Defense Technical Information Center   2
   8725 John J. Kingman Rd., STE 0944
   Ft. Belvoir, VA 22060-6218

2. Dudley Knox Library   2
   Naval Postgraduate School
   411 Dyer Rd.
   Monterey, CA 93943-5101

3. Chairman, Code ME   1
   Department of Mechanical Engineering
   Naval Postgraduate School
   Monterey, CA 93943-5000

4. Professor Ashok Gopinath, Code ME/GK   2
   Department of Mechanical Engineering
   Naval Postgraduate School
   Monterey, CA 93943-5000

5. Naval Engineering Curricular Office, Code 34   1
   Naval Postgraduate School
   Monterey, CA 93943-5000

6. Deniz Kuvvetleri Komutanlığı   2
   Personel Daire Başkanlığı
   Bakanlıklar, Ankara, Turkey

7. Deniz Harp Okulu Komutanlığı   1
   Tuzla, İstanbul, Turkey 81704

8. Birol Zeybek   2
   4 Eylül Mah., Hasan Polatkan Cd.
   Elif Apt. No.25/6
   Tire, İzmir, Turkey 35900

9. İ. T. Ü. Makina Müh. Bl.   1
   Ratip Berker Kütüphanesi
   Maslak, İstanbul, Turkey

10.   Murat Kocakanat
              Yüzbaşılar Mah., İstiklal Cd.
              No.31/10
              Değirmendere, Kocaeli, TURKEY 41950   1